JOURNAL OF GUIDANCE, CONTROL, AND DYNAMICS
Vol. 27, No. 5, September–October 2004

Aeroelasticity of Time-Delayed Feedback Control of Two-Dimensional Supersonic Lifting Surfaces

Yuan Yuan*
Memorial University of Newfoundland, St. John's, Newfoundland A1C 5S7, Canada
Pei Yu†
The University of Western Ontario, London, Ontario N6A 5B7, Canada
Liviu Librescu‡
Virginia Polytechnic Institute and State University, Blacksburg, Virginia 24061-0219
and
Piergiovanni Marzocca§
Clarkson University, Potsdam, New York 13699-5725

Determination of the nature of the critical flutter boundary (benign/catastrophic) and its control constitute important issues that can be addressed within the nonlinear formulation of lifting surface theory. The main attention of this paper consists in the development of a computational approach enabling one to get a better understanding on time-delayed dynamics as applied to this important aeroelastic problem, and more specifically, to two-dimensional supersonic lifting surfaces. The analysis is based on the reduction of the infinite-dimensional problem to one described on a two-dimensional center manifold. Results presenting the implication of the linear/nonlinear time-delayed feedback control on two-dimensional supersonic lifting surfaces are addressed, and pertinent conclusions are drawn.

Nomenclature

A, A^*	=	linear operator and its dual operator, respectively
a_i, b_i, e_i, f_i	=	coefficients appearing in Eq. (7)
B	=	normalized nonlinear stiffness coefficient in pitch
b	=	semichord length
C_{ij}	=	coefficient of third-order polynomial in $\mathcal{N}$
c_h, c_α	=	linear viscous damping coefficients in plunging and pitching, respectively
$D(\lambda)$	=	characteristic equation
F	=	nonlinear function
H, H^*	=	Banach space and its dual, respectively
h, ξ	=	plunging displacement and its dimensionless counterpart ($\equiv h/b$), respectively
I_α	=	mass moment of inertia per unit span
K_h, K_α	=	linear stiffness coefficients in plunging and pitching, respectively
L	=	Lyapunov coefficient
$\mathcal{L}$, $\mathcal{M}$	=	dimensionless unsteady lift and moment per unit wing span
M_∞, (M_{TR})	=	undisturbed (transitory) flight Mach number ($\equiv U_\infty/a_\infty$)
m	=	airfoil mass per unit span
$\mathcal{N}$	=	nonlinear terms on center manifold
P_Λ	=	two-dimensional space spanned by the eigenvectors of operator A associated with the eigenvalues Λ
Q_Λ	=	complementary space of P_Λ
q	=	complex eigenvector corresponding to A and $i\omega$
q^*	=	complex eigenvector corresponding to A^* and $-i\omega$
r	=	phase variable in normal form
r_α	=	dimensionless radius of gyration with respect to the elastic axis, [$\equiv \sqrt{(I_\alpha/mb^2)}$]
S_α, χ_α	=	static unbalance about the elastic axis and its dimensionless counterpart,($\equiv S_\alpha/mb$), respectively
$\hat{t}$, t	=	time variable and its dimensionless counterpart, ($\equiv U_\infty \hat{t}/b$), respectively
U_∞, V	=	freestream speed and its dimensionless counterpart, ($\equiv U_\infty/b\omega_\alpha$), respectively
V_F	=	normalized flutter speed, ($U_F/b\omega_\alpha$)
$\boldsymbol{w}$	=	local coordinate system on center manifold induced by base Ψ
x_{ea}, x_0	=	elastic axis position and its dimensionless counterpart ($\equiv x_{\mathrm{ea}}/b$), respectively, measured from the leading edge (positive aft)
α	=	twist angle about the pitch axis
γ	=	aerodynamic correction factor
δ_A	=	tracing quantities identifying the aerodynamic nonlinear term
ζ_h, ζ_α	=	damping ratios in plunging ($\equiv c_h/2m\omega_h$) and pitching ($\equiv c_\alpha/2I_\alpha\omega_\alpha$), respectively
θ	=	frequency variable in normal form
κ	=	polytropic gas coefficient
μ	=	dimensionless mass ratio, ($\equiv m/4\rho_\infty b^2$)
ρ_∞, a_∞	=	air density and the speed of sound of the undisturbed flow, respectively
$\hat{\tau}$, τ	=	time delay and its dimensionless counterpart, ($\equiv \hat{\tau}\omega_\alpha$), respectively
$\Phi(\theta)$, $\Psi(\theta)$	=	real basis for P_Λ and Q_Λ, respectively
Ψ_1, Ψ_2	=	linear and nonlinear normalized control gains, respectively
Ψ^T	=	transpose of Ψ

Presented as Paper 2003-1733 at the AIAA/ASME/ASCE/AHS/ASC 44th Structures, Structural dynamics, and Materials Conference, Norfolk, VA, 7–10 April 2003; received 29 June 2003; revision received 9 December 2003; accepted for publication 9 December 2003.

*Assistant Professor, Department of Mathematics and Statistics.
†Professor, Department of Applied Mathematics.
‡Professor, Department of Engineering Science and Mechanics.
§Assistant Professor, Department of Mechanical and Aeronautical Engineering. Member AIAA.

ω	=	value of the pure imaginary roots of $D(\lambda)$ in Eq. (10)
ω_h, ω_α, $\bar{\omega}$	=	uncoupled frequencies of linearized aeroelastic system counterpart in plunging, $[\equiv \sqrt{(K_h/m)}]$, pitching $[\equiv \sqrt{(K_h/I_\alpha)}]$ and frequency ratio $(\equiv \omega_h/\omega_\alpha)$, respectively
$(\dot{\ })$	=	$\mathrm{d}(\,)/\mathrm{d}t$

Introduction

BECAUSE of its evident practical importance, the study of the flutter instability of flight vehicle constitutes an essential prerequisite in their design process. The flutter instability can jeopardize aircraft performance and dramatically affect its survivability. Moreover, the tendency of increasing structural flexibility and maximum operating speed increase the likelihood of the flutter occurrence within the aircraft operational envelope. As a result of the considerable importance of this problem, a great deal of research activity devoted to the aeroelastic active control and flutter suppression of flight vehicles was carried out. In this sense, the reader is referred to a sequence of issues in Refs. 1 and 2, where valuable contributions to this topic have been supplied.

As it clearly appears, within this problem, two principal issues deserve special attention: 1) increase, without weight penalties, of the flutter speed, and 2) possibilities to convert unstable limit cycles into stable ones. While the achievement of 1) can result in the expansion of the flight envelope, which related with 2) would result in the possibility to operate in close proximity of the flutter boundary without the danger of encountering the catastrophic flutter instability, but in the worst possible scenario, crossing the flutter boundary that features a benign character. In contrast to the catastrophic flutter boundary in which case the amplitude of oscillations increases exponentially, in the case of benign flutter boundary, monotonic increase of the oscillation amplitude occurs, and, as a result, the failure can occur only by fatigue. It clearly appears that both issues 1) and 2) are related to controlling Hopf bifurcations. In particular, issue 1) implies increase of the stability of an equilibrium and delay of the occurrence of Hopf bifurcations[3–6] whereas issue 2) is related to controlling Hopf bifurcations once a periodic vibration has been initiated.[7,8] Recently, a new control method for Hopf bifurcation has been proposed, and both of the two issues are discussed.[9]

This present study primarily deals with the determination and control of the flutter instability and of the character of the flutter boundary of supersonic/hypersonic lifting surfaces. This implies the determination of the conditions generating the catastrophic type of flutter boundary and implementation of an active control capability enabling one to convert this type of flutter boundary into a benign one. This issue is of a considerable importance toward the expansion, without catastrophic failures, of the flight envelope of the vehicle. In contrast to the issue of the determination of the flutter boundary that requires a linearized analysis, the problem of the determination of the character of the flutter boundary requires a nonlinear approach. As it has been shown,[10–13] at hypersonic speeds the aerodynamic nonlinearities play a detrimental role, in the sense that they contribute to conversion of the benign flutter boundary to a catastrophic one. Therefore, an active control capability enabling one to prevent conversion of the flutter boundary into a catastrophic one should be implemented.

Aeroelastic Model

This investigation is based on a geometrical and aerodynamic nonlinear model of a wing section of the high-speed aircraft incorporating an active control capability. The geometry of the model is shown in Fig. 1. As concerns the nonlinear unsteady aerodynamic lift and moment, these are obtained through the integration of the pressure difference and of its moment with respect to the pitching axis, respectively, on the upper and lower surfaces of the airfoil. To this end, the third-order approximation of the piston theory

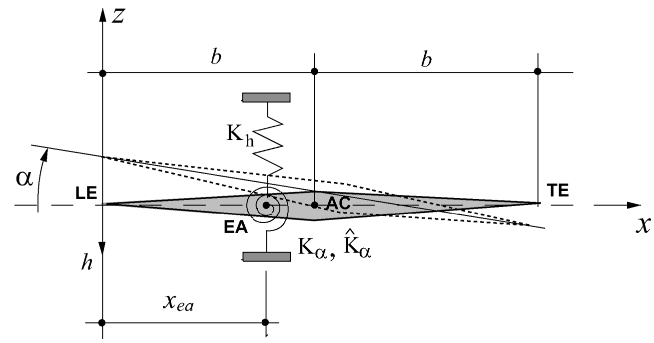

Fig. 1 Geometry of the cross section of lifting surface.

aerodynamics[10–15] (PTA), as given by

$$p(x,t) = p_\infty\left\{1 + \kappa(\nu_z/a_\infty)\gamma + [\kappa(\kappa+1)/4][(\nu_z/a_\infty)\gamma]^2 + [\kappa(\kappa+1)/12][(\nu_z/a_\infty)\gamma]^3\right\} \tag{1}$$

is considered. Herein

$$\nu_z = -\left(\frac{\partial w}{\partial t} + U_\infty\frac{\partial w}{\partial x}\right)\operatorname{sgn} z \tag{2}$$

denotes the downwash velocity normal to the lifting surface $a_\infty^2 = \kappa p_\infty/\rho_\infty$, where $\operatorname{sgn} z$ assumes the value 1 or -1 for $z > 0$ and $z < 0$, respectively. In addition,

$$w(t) = h(t) + \alpha(t)(x - bx_0) \tag{3}$$

denotes the transversal displacement of the elastic surface; $x_0(\equiv x_{\mathrm{ea}}/b)$ is the dimensionless streamwise position of the pitch axis measured from the leading edge; p_∞, ρ_∞, U_∞, and a_∞ are the pressure, the air density, the airflow speed, and the speed of sound of the undisturbed flow, respectively; and $\gamma = M_\infty/\sqrt{(M_\infty^2 - 1)}$ is an aerodynamic correction factor that enables one to extend the validity of the PTA to the entire low-supersonic/hypersonic-speed range.

In the context of the inclusion of the structural and aerodynamic nonlinearities, of the linear and nonlinear controls and of the associated time delay, in conjunction with the typical cross section with pitch-and-plunge degrees of freedom, the dimensionless aeroelastic equations representing an extension of those in Refs. 3 and 16 are written as

$$\ddot{\xi} + \chi_\alpha\ddot{\alpha} + 2\zeta_h(\bar{\omega}/V)\dot{\xi} + (\bar{\omega}/V)^2\xi = \mathcal{L}(t) \tag{4a}$$

$$\left(\chi_\alpha/r_\alpha^2\right)\ddot{\xi} + \ddot{\alpha} + (2\zeta_\alpha/V)\dot{\alpha} + (1/V^2)\alpha + (1/V^2)B\alpha^3 = \mathcal{M}(t) - \left(\Psi_1/V^2\right)\alpha(t-\tau) - \left(\Psi_2/V^2\right)\alpha^3(t-\tau) \tag{4b}$$

where

$$\mathcal{L}(t) = -(\gamma/12\mu M_\infty)\left\{12\alpha + \delta_A M_\infty^2(1+\kappa)\gamma^2\alpha^3 + 12[\dot{\xi} + \dot{\alpha}(b - x_{\mathrm{ea}})/b]\right\} \tag{5a}$$

$$\mathcal{M}(t) = -(\gamma/12\mu M_\infty)\left(1/r_\alpha^2 b\right)\left\{12(b - x_{\mathrm{ea}})\alpha + \delta_A M_\infty^2(b - x_{\mathrm{ea}})(1+\kappa)\gamma^2\alpha^3 + 4\left[3(b - x_{\mathrm{ea}})\dot{\xi} + \dot{\alpha}\left(4b^2 - 6bx_{\mathrm{ea}} + 3x_{\mathrm{ea}}^2\right)/b\right]\right\} \tag{5b}$$

and $\xi(t) = h(t)/b$, $\alpha(t)$ is the twist angle about the pitch axis, and $\mathcal{L}(t)$ and $\mathcal{M}(t)$ denote the dimensionless aerodynamic lift and moment, respectively. The meaning of the remaining parameters can be found in the nomenclature (see also Refs. 3, 10, and 16). In Eq. (4b), the parameter B identifies the nature of the structural nonlinearity of the system in the sense that, corresponding to $B < 0$ or $B > 0$, the structural nonlinearities are soft or hard, respectively, whereas for $B = 0$ the system is structurally linear. The linear and nonlinear active controls are given in terms of two normalized control gain parameters Ψ_1 and Ψ_2, respectively.

A mathematical model is generally the first approximation of the considered real system. More realistic models should include some of the past states of the system, that is, the model should include time delay. The time delay in control can occur either beyond our will or it can be designed as to modify the performance of the system.[11] For this reason, as a necessary prerequisite, a good understanding of its effects on the flutter instability boundary and its character (benign or catastrophic) is required.

Linear/Nonlinear Stability Analysis

State-Space Form of Aeroelastic Equations

To capture the effect of time delay τ, introduced in the related terms Ψ_1 and Ψ_2, let $\xi = x_1$, $\alpha = x_2$, $\dot{\xi} = x_3$, $\dot{\alpha} = x_4$, and $x_{2t} = x_2(t-\tau)$. Then, one can rewrite Eqs. (4a) and (4b) as a set of four first-order differential equations:

$$\dot{x_1} = x_3 \tag{6a}$$

$$\dot{x_2} = x_4 \tag{6b}$$

$$\dot{x_3} = a_1x_1 + a_2x_2 + a_3x_3 + a_4x_4 + a_5x_2^3 + e_1x_{2t} + e_2x_{2t}^3 \tag{6c}$$

$$\dot{x_4} = b_1x_1 + b_2x_2 + b_3x_3 + b_4x_4 + b_5x_2^3 + f_1x_{2t} + f_2x_{2t}^3 \tag{6d}$$

where all of the coefficients that are provided in Appendix A are explicitly expressed in terms of the parameters of Eqs. (4a) and (4b).

For convenience in the following analysis, rewrite Eqs. (6a–6d) in the vector form:

$$\dot{\boldsymbol{x}}(t) = A_1\boldsymbol{x}(t) + A_2\boldsymbol{x}(t-\tau) + \boldsymbol{F}[\boldsymbol{x}(t), \boldsymbol{x}(t-\tau)] \tag{7}$$

where $\boldsymbol{x}, \boldsymbol{F} \in R^4$, A_1, and A_2 are 4×4 matrices. A_1, A_2, and $\boldsymbol{F}$ are given by

$$A_1 = \begin{bmatrix} 0 & 0 & 1 & 0 \\ 0 & 0 & 0 & 1 \\ a_1 & a_2 & a_3 & a_4 \\ b_1 & b_2 & b_3 & b_4 \end{bmatrix} \tag{8a}$$

$$A_2 = \begin{bmatrix} 0 & 0 & 0 & 0 \\ 0 & 0 & 0 & 0 \\ 0 & e_1 & 0 & 0 \\ 0 & f_1 & 0 & 0 \end{bmatrix} \tag{8b}$$

and

$$\boldsymbol{F} = \begin{pmatrix} 0 \\ 0 \\ a_5x_2^3(t) + e_2x_2^3(t-\tau) \\ b_5x_2^3(t) + f_2x_2^3(t-\tau) \end{pmatrix} \tag{8c}$$

respectively.

Hopf bifurcation has been extensively studied using many different methods,[3–5] for example, Lyapunov quantity used in the context of the supersonic panel flutter,[12,13] where the effects of structural, aerodynamical, and physical nonlinearities have been incorporated. In Refs. 11 and 16, the dynamic behavior of the system without time delay in the control was studied in the vicinity of a Hopf bifurcation critical point. In particular, the effect of the active control on the character of the flutter boundary (where the Jacobian has a purely imaginary pair) is investigated. It is shown that for different flight speeds, stable (unstable) equilibrium and stable (unstable) limit cycles exist.

The effect of the time delay involved in the feedback control will be considered in this paper. Nonlinear systems involving time delay have been studied by many authors.[7,17,18] In the past two decades, there has been rapidly growing interest in bifurcation control.[7–9] There are a wide variety of promising potential applications of bifurcation and chaos control. In general, the aim of bifurcation control is to design a controller such that the bifurcation characteristics of a nonlinear system undergoing bifurcations can be modified to achieve some desirable dynamical behaviors, such as changing a subcritical Hopf bifurcation to supercritical, eliminating chaotic motions, etc. In this context, many applications have been found, for example, in the areas of mechanical systems, fluid dynamics, biological systems, and secure communications. The approach developed in Ref. 18 will be applied to study the effect of the time delay involved in the feedback control. The main attention is focused on Hopf bifurcation.

Linearized System

As the first step, we analyze the stability of the trivial solution of the linearized system of Eq. (7), which is given by

$$\dot{\boldsymbol{x}}(t) = A_1\boldsymbol{x}(t) + A_2\boldsymbol{x}(t-\tau) \qquad \boldsymbol{x} \in R^4 \tag{9}$$

The characteristic function can be obtained by substituting the trial solution $\boldsymbol{x}(t) = \boldsymbol{c}e^{\lambda t}$, where $\boldsymbol{c}$ is a constant vector, into the linear part to find

$$\begin{aligned} D(\lambda) &= \det\left(\lambda I - A_1 - A_2e^{-\lambda\tau}\right) = \lambda^4 - (a_3+b_3)\lambda^3 \\ &\quad + (a_3b_4 - a_4b_3 - b_2 - a_1)\lambda^2 + (b_2a_3 - b_3a_2 + a_1b_4 - b_1a_4)\lambda \\ &\quad + a_1b_2 - a_2b_1 - \left[f_1\lambda^2 + (b_3e_1 - a_3f_1)\lambda + (b_1e_1 - a_1f_1)\right]e^{-\lambda\tau} \end{aligned} \tag{10}$$

where I denotes the identity matrix. It can be shown[18] that the number of the eigenvalues of the characteristic equation (10) with negative real parts, counting multiplicities, can change only when the eigenvalues become pure imaginary pairs as the time delay τ and the components of A_1 and A_2 are varied.

It is seen from Eq. (10) that when $a_1(b_2+f_1) \neq b_1(a_2+e_1)$ none of the roots of $D(\lambda)$ is zero. Thus, the trivial equilibrium $\boldsymbol{x} = 0$ becomes unstable only when Eq. (10) has at least a pair of purely imaginary roots $\lambda = \pm i\omega$ (i is the imaginary unit), at which a Hopf bifurcation occurs. The critical value for the Hopf bifurcation to occur can be found from the equation

$$\begin{aligned} D(i\omega) &= \Big[\left(f_1\omega^2 + a_1f_1 - b_1e_1\right)\cos(\omega\tau) + \omega(f_1a_3 - b_3e_1)\sin(\omega\tau) \\ &\quad + \omega^4 + (b_2 + a_1 - a_3b_4 + a_4b_3)\omega^2 + a_1b_2 - b_1a_2\Big] \\ &\quad + \Big[\omega(f_1a_3 - b_3e_1)\cos(\omega\tau) - \left(a_1f_1 + f_1\omega^2 - b_1e_1\right)\sin(\omega\tau) \\ &\quad + (a_4+b_3)\omega^3 + (b_2a_3 - b_3a_2 + a_1b_4 - b_1a_4)\omega\Big]i \end{aligned} \tag{11}$$

Setting the real and imaginary parts in Eq. (11) to zero results in

$$\cos(\omega\tau) = P_1/P \qquad \text{and} \qquad \sin(\omega\tau) = P_2/P \tag{12}$$

where

$$\begin{aligned} P_1 &= -f_1\omega^6 + \left(a_3b_3e_1 + b_4b_3e_1 - f_1a_4b_3 - a_3^2f_1 + b_1e_1\right. \\ &\quad \left. - 2f_1a_1 - f_1b_2\right)\omega^4 + \left(a_1b_4b_3e_1 + b_1a_4f_1a_3 + b_2a_3b_3e_1\right. \\ &\quad - b_3^2a_2e_1 - b_2a_3^2f_1 - b_1e_1a_3b_4 + b_3a_2f_1a_3 - a_1f_1a_4b_3 \\ &\quad \left. - 2f_1a_1b_2 + f_1b_1a_2 + b_1e_1b_2 + b_1e_1a_1 - a_1^2f_1\right)\omega^2 \\ &\quad + (a_1f_1 - b_1e_1)(b_1a_2 - a_1b_2) \end{aligned} \tag{13a}$$

$$\begin{aligned} P_2 &= \omega\Big[(f_1b_4 + b_3e_1)\omega^4 + \big(f_1b_4a_3^2 - f_1a_3a_4b_3 - f_1b_1a_4 \\ &\quad - f_1b_3a_2 + 2f_1a_1b_4 - b_1e_1a_3 - a_3b_4b_3e_1 + b_2b_3e_1 - b_1e_1b_4 \\ &\quad + a_1b_3e_1 + a_4b_3^2e_1\big)\omega^2 + b_1a_4(b_1e_1 - a_1f_1)\Big] \\ &\quad + a_1f_1(a_1b_4 - a_2b_3) + a_3b_1(f_1a_2 - e_1b_2) \\ &\quad + a_1e_1(b_2b_3 - b_1b_4) \end{aligned} \tag{13b}$$

$$\begin{aligned} P &= f_1^2\omega^4 + \left[(b_3e_1 - f_1a_3)^2 + 2f_1(f_1a_1 - b_1e_1)\right]\omega^2 \\ &\quad + (b_1e_1 - a_1f_1)^2 \end{aligned} \tag{13c}$$

With the aid of Eqs. (12) and (13a–13c), one uses equation $\sin^2(\omega\tau)+\cos^2(\omega\tau)=1$ to obtain the following eighth-degree characteristic polynomial for solving the critical values of ω:

$$\omega^8 + q_1\omega^6 + q_2\omega^4 + q_3\omega^2 + q_4 = 0 \tag{14}$$

where

$$q_1 = a_3^2 + b_4^2 + 2(b_2 + a_4 b_3 + a_1) \tag{15a}$$

$$\begin{aligned} q_2 = {} & (a_1+b_1)^2 + (a_3b_4 - a_4b_3)^2 - f_1^2 + 2[a_3(b_2a_3 - a_2b_3) \\ & + a_4(a_1b_4 - b_1a_3)] + 2[b_3(a_4b_2 - a_2b_4) + b_4(a_1b_4 - b_1a_4)] \end{aligned} \tag{15b}$$

$$\begin{aligned} q_3 = {} & (a_1b_4 - a_4b_1)^2 + (a_2b_3 - a_3b_2)^2 - (a_3f_1 - b_3e_1)^2 \\ & + 2(a_4b_2 - a_2b_4)(a_1b_3 - a_3b_1) + 2[(a_1+b_1)(a_1b_2 - a_2b_1) \\ & + f_1(b_1e_1 - f_1a_1)] \end{aligned} \tag{15c}$$

$$q_4 = (a_1b_2 - a_2b_1)^2 - (a_1f_1 - b_1e_1)^2 \tag{15d}$$

If Eq. (14) has no positive real roots (for ω^2), then system (9) does not contain center manifold, but stable and unstable manifolds. On the other hand, if Eq. (14) has at least one positive solution for ω, one can substitute the solution(s) into Eq. (11) to find the smallest $\tau_{\min}$, at which the system undergoes a Hopf bifurcation.

Although a closed-form solution exists for the roots of a general fourth-degree polynomial [consider Eq. (14) as a fourth-degree polynomial of ω^2], it is not useful here in finding the relations between the parameters because the expressions are too involved. In this paper, we will use a numerical approach to find the relations among the flutter speed $V_F(\equiv U_F/b\omega_\alpha)$, flight Mach Number M_∞, time delay τ, and the control gains Ψ_1, Ψ_2. More computation results will be given in the Results section.

Center Manifold Reduction

To obtain the explicit analytical expressions for the stability condition of Hopf bifurcation solutions (limit cycles), system (4) should be reduced to its center manifold.[18] While studying the critical infinite dimensional problem on a two-dimensional center manifold, we express the delay equation as an abstract evolution equation on Banach space H of continuously differentiable function $\boldsymbol{u}: [-\tau, 0] \to R^2$ as

$$\dot{\boldsymbol{x}} = A\boldsymbol{x}_t + \boldsymbol{F}(t, \boldsymbol{x}_t) \tag{16}$$

where $\boldsymbol{x}_t(\theta) = \boldsymbol{x}(t+\theta)$ for $-\tau \le \theta \le 0$ and A is a linear operator for the critical case, expressed by

$$A\boldsymbol{u}(\theta) = \begin{cases} \dfrac{\mathrm{d}\boldsymbol{u}(\theta)}{\mathrm{d}\theta} & \text{for} \quad \theta \in [-\tau, 0) \\ A_1\boldsymbol{u}(0) + A_2\boldsymbol{u}(-\tau) & \text{for} \quad \theta = 0 \end{cases} \tag{17}$$

The nonlinear operator F is in the form of

$$\boldsymbol{F}(\boldsymbol{u})(\theta) = \begin{cases} 0 & \text{for} \quad \theta \in [-\tau, 0) \\ \boldsymbol{F}[\boldsymbol{u}(0), \boldsymbol{u}(-\tau)] & \text{for} \quad \theta = 0 \end{cases} \tag{18}$$

Similarly, we can define the dual/adjoint space H^* of continuously differentiable function $\boldsymbol{v}: [0, \tau] \to R^2$ with the dual operator

$$A^*\boldsymbol{v}(\sigma) = \begin{cases} -\dfrac{\mathrm{d}\boldsymbol{v}(\sigma)}{\mathrm{d}\sigma} & \text{for} \quad \sigma \in (0, \tau] \\ A_1^*\boldsymbol{v}(0) + A_2^*\boldsymbol{v}(\tau) & \text{for} \quad \sigma = 0 \end{cases} \tag{19}$$

From the discussion given in the preceding subsection, we know that the characteristic equation (10) has a single pair of purely imaginary eigenvalues $\Lambda = \pm i\omega$. Therefore, H can be split into two subspaces as $H = P_\Lambda \oplus Q_\Lambda$, where P_Λ is a two-dimensional space spanned by the eigenvectors of the operator A associated with the eigenvalues Λ, while Q_Λ is the complementary space of P_Λ. Then for $\boldsymbol{u} \in H$ and $\boldsymbol{v} \in H^*$, we can define a bilinear operator:

$$\begin{aligned} \langle \boldsymbol{v}, \boldsymbol{u} \rangle &= \bar{\boldsymbol{v}}^T(0)\boldsymbol{u}(0) - \int_{-\tau}^{0}\int_{0}^{\theta} \bar{\boldsymbol{v}}^T(\xi - \theta)[\mathrm{d}\eta(\theta)]\boldsymbol{u}(\xi)\,\mathrm{d}\xi \\ &= \bar{\boldsymbol{v}}^T(0)\boldsymbol{u}(0) + \int_{-\tau}^{0} \bar{\boldsymbol{v}}^T(\xi + \theta)A_2(\xi)\boldsymbol{u}(\xi)\,\mathrm{d}\xi \end{aligned} \tag{20}$$

Corresponding to the critical characteristic root $i\omega$, the complex eigenvector $\boldsymbol{q}(\theta) \in H$ satisfies

$$\frac{\mathrm{d}\boldsymbol{q}(\theta)}{\mathrm{d}\theta} = i\omega\boldsymbol{q}(\theta), \qquad \text{for} \qquad \theta \in [-\tau, 0) \tag{21a}$$

$$A_1\boldsymbol{q}(0) + A_2\boldsymbol{q}(-\tau) = i\omega\boldsymbol{q}(0), \qquad \text{for} \qquad \theta = 0 \tag{21b}$$

The general solution of Eqs. (21a) and (21b) is

$$\boldsymbol{q}(\theta) = \boldsymbol{C}e^{i\omega\theta} \tag{22}$$

From the boundary conditions [given in Eq. (17) when $\theta = 0$] we find the following matrix equation:

$$\begin{bmatrix} -i\omega & 0 & 1 & 0 \\ 0 & -i\omega & 0 & 1 \\ a_1 & a_2 + e_1e^{-i\omega\tau} & a_3 - i\omega & a_4 \\ b_1 & b_2 + f_1e^{-i\omega\tau} & b_3 & b_4 - i\omega \end{bmatrix} \boldsymbol{C} = 0 \tag{23}$$

By letting $\boldsymbol{C} = (C_1, C_2, C_3, C_4)^T$ and choosing $C_1 = 1$, we uniquely determine C_2, C_3, and C_4. Then the eigenvector $\boldsymbol{q}(\theta) = \boldsymbol{C}e^{i\omega\theta}$ is found. Thus, the real basis for P_Λ is obtained as $\Phi(\theta) = (\varphi_1, \varphi_2) = (\mathrm{Re}[\boldsymbol{q}(\theta)], \mathrm{Im}[\boldsymbol{q}(\theta)])$, that is,

$$\Phi(\theta) = \begin{bmatrix} \cos(\omega\theta) & \sin(\omega\theta) \\ \dfrac{L_1\cos(\omega\theta) + \omega L_2\sin(\omega\theta)}{L_0} & \dfrac{L_1\sin(\omega\theta) - \omega L_2\cos(\omega\theta)}{L_0} \\ -\omega\sin(\omega\theta) & \omega\cos(\omega\theta) \\ \dfrac{\omega[\omega L_2\cos(\omega\theta) - L_1\sin(\omega\theta)]}{L_0} & \dfrac{\omega[\omega L_2\sin(\omega\theta) + L_1\cos(\omega\theta)]}{L_0} \end{bmatrix} \tag{24}$$

where explicit expressions of L_i $(i = 0, 1, 2)$ are provided in Appendix B.

Similarly, from the equation

$$A^*\boldsymbol{q}^*(\sigma) = -i\omega\boldsymbol{q}^*(\sigma)$$

or

$$-\frac{\mathrm{d}\boldsymbol{q}^*(\sigma)}{\mathrm{d}\sigma} = -i\omega\boldsymbol{q}^*(\sigma) \qquad \text{for} \qquad \sigma \in [0, \tau)$$

$$A_1^*\boldsymbol{q}^*(0) + A_2^*\boldsymbol{q}^*(\tau) = -i\omega\boldsymbol{q}^*(0) \qquad \text{for} \qquad \sigma = 0 \tag{25}$$

one can choose the real basis for the dual space Q_Λ as $\Psi(\sigma) = (\psi_1, \psi_2) = (Re[\boldsymbol{q}^*(\sigma)], \mathrm{Im}[\boldsymbol{q}^*(\sigma)])$, that is,

$$\Psi(\sigma) = \begin{bmatrix} \dfrac{L_3\cos(\omega\sigma) + L_4\sin(\omega\sigma)}{M} & \dfrac{L_3\sin(\omega\sigma) - L_4\cos(\omega\sigma)}{M} \\ \dfrac{L_5\cos(\omega\sigma) + L_6\sin(\omega\sigma)}{M} & \dfrac{L_5\sin(\omega\sigma) - L_6\cos(\omega\sigma)}{M} \\ \dfrac{L_7\cos(\omega\sigma) + L_8\sin(\omega\sigma)}{M} & \dfrac{L_7\sin(\omega\sigma) - L_8\cos(\omega\sigma)}{M} \\ N_1\cos(\omega\sigma) - N_2\sin(\omega\sigma) & N_1\sin(\omega\sigma) + N_2\cos(\omega\sigma) \end{bmatrix} \tag{26}$$

where the explicit expressions of $L_i (i = 3, \ldots, 8)$ and M are also provided in Appendix B, and N_1 and N_2 can be obtained from the relation $\langle \Psi, \Phi \rangle = I$, expressed in terms of ω, τ, and the coefficients a_i, b_i, e_i, and f_i in Eqs. (6a–6d). The lengthy expressions of N_1 and N_2 are omitted here.

Next, by defining $\boldsymbol{w} \equiv (w_1, w_2)^T = \langle \Psi, \boldsymbol{u}_t \rangle$ (which actually represents the local coordinate system on the two-dimensional center manifold, induced by the basis Ψ), with the aid of Eqs. (24) and (26), one can decompose $\boldsymbol{u}_t$ into two parts to obtain

$$\boldsymbol{u}_t = \boldsymbol{u}_t^{P_\Lambda} + \boldsymbol{u}_t^{Q_\Lambda} = \Phi \langle \Psi, \boldsymbol{u}_t \rangle + \boldsymbol{u}_t^{Q_\Lambda} = \Phi \boldsymbol{w} + \boldsymbol{u}_t^{Q_\Lambda} \tag{27}$$

which implies that the projection of $\boldsymbol{u}_t$ on the center manifold is $\Phi \boldsymbol{w}$. Then, applying Eqs. (16) and (27) results in

$$\left\langle \Psi, \Phi \dot{\boldsymbol{w}} + \dot{\boldsymbol{u}}_t^Q \right\rangle = \left\langle \Psi, A\left(\Phi \boldsymbol{w} + \boldsymbol{u}_t^Q\right) \right\rangle + \left\langle \Psi, F\left(\boldsymbol{t}, \Phi \boldsymbol{w} + \boldsymbol{u}_t^Q\right) \right\rangle \tag{28}$$

and therefore,

$$\langle \Psi, \Phi \rangle \dot{\boldsymbol{w}} = \langle \Psi, A\Phi \rangle \boldsymbol{w} + \left\langle \Psi, \boldsymbol{F}\left(\boldsymbol{t}, \Phi \boldsymbol{w} + \boldsymbol{u}_t^Q\right) \right\rangle$$

which can be written as $I\dot{\boldsymbol{w}} = D_\Lambda \boldsymbol{w} + \mathcal{N}(\boldsymbol{w})$, and finally we obtain the equation of the center manifold:

$$\dot{\boldsymbol{w}} = \begin{bmatrix} 0 & \omega \\ -\omega & 0 \end{bmatrix} \boldsymbol{w} + \mathcal{N}(\boldsymbol{w}) \tag{29}$$

where $\mathcal{N}(\boldsymbol{w})$ represents the nonlinear terms contributed from the original system to the center manifold.

The lowest-order nonlinear terms of the center manifold, needed to determine the solutions, are

$$\begin{aligned} \mathcal{N}_3(\boldsymbol{w}) &= \Psi^T(0) F(\Phi \boldsymbol{w}) \\ &= \Psi^T(0) \begin{pmatrix} 0 \\ 0 \\ a_5 \hat{a}_1 + e_2 \hat{a}_2 \\ b_5 \hat{a}_1 + f_2 \hat{a}_2 \end{pmatrix} \\ &= \begin{pmatrix} C_{30}^1 w_1^3 + C_{21}^1 w_1^2 w_2 + C_{12}^1 w_1 w_2^2 + C_{03}^1 w_2^3 \\ C_{30}^1 w_2^3 + C_{21}^2 w_1^2 w_2 + C_{12}^2 w_1 w_2^2 + C_{03}^2 w_2^3 \end{pmatrix} \end{aligned} \tag{30}$$

where in $\hat{a}_1 = [\Phi(0) w]_2^3$ and $\hat{a}_2 = [\Phi(-\tau) w]_2^3$, "$[\cdots]_2^3$" denotes the cubic order terms extracted from the second component of the vector ( ). In fact, because Φ is a 4×2 matrix and $\boldsymbol{w}$ is a 2×1 vector, $\Phi\, \boldsymbol{w}$ is a 4×1 vector, which can include higher-order terms in the components; we just intercept the third-order terms. Therefore, we obtain the normal form up to third order by using the method developed in Ref. 6,

$$\dot{r} = Lr^3, \qquad \dot{\theta} = \omega + br^2 \tag{31}$$

where L is a Lyapunov coefficient, also referred to as Lyapunov first quantity (LFQ), given by

$$L = \tfrac{1}{8}\left(3C_{30}^1 + C_{12}^1 + C_{21}^2 + 3C_{03}^2\right) \tag{32}$$

When $L < 0 (>0)$, the Hopf bifurcation is supercritical (subcritical), that is, the bifurcating limit cycle is stable (unstable).

Results

In this section, some numerical results are presented to investigate the stability with respect to the choices of the time delay τ and the linear and nonlinear control gains Ψ_1 and Ψ_2 using the formulas presented in the preceding section.

To compare the results with those in Ref. 16 where the approach of Refs. 12 and 13 was used and no time delay was presented, we shall take the same parameter values used in Ref. 16. The main chosen varying parameters are M_∞, Ψ_1, Ψ_2, and time delay τ, while other parameters given in Eqs. (4a) and (4b) are fixed:

$$\begin{gathered} b = 1.5\ \mathrm{m(dimensional)}, \qquad \mu = 50, \qquad \bar{\omega} = 1.0 \\ r_\alpha = 0.5, \qquad \chi_\alpha = 0.25 \\ \gamma = 1, \qquad \zeta_h = \zeta_\alpha = 0, \qquad \kappa = 1.4, \qquad \delta_A = 1, \qquad B = 1 \\ x_0 = 0.5, \qquad \omega_\alpha = 60 \end{gathered} \tag{33}$$

The stability of the aeroelastic system in the vicinity of the flutter boundary is analyzed on the basis of Eqs. (24) and (26).

We know from Ref. 16 that when either the linear or the nonlinear control gain is added at relatively moderate supersonic flight Mach numbers the flutter boundary is benign, whereas with the increase of the flight Mach number, because of the built-up aerodynamic nonlinearities that become prevalent, the flutter boundary becomes catastrophic. Here, we will show how the stability changes when the time delay is included.

Three typical cases are discussed next. Note that in the discussions V_F denotes the flutter velocity at which Hopf bifurcation (caused by flutter instability) is initiated, leading to periodic motions. The stability of the bifurcating limit cycle is determined by the sign of L, the Lyapunov coefficient. The computation of L is based on the center manifold and Eq. (29) described in the preceding section.

Case 1: No delay (i.e., $\tau = 0$), Ψ_1 is varied.

a) $\Psi_2 = 0$ (nonlinear feedback control is not applied). Consider the linear feedback control with gain Ψ_1, but without the time delay. The results of the flutter velocity with respect to flight Mach number for different values of Ψ_1 and the corresponding Lyapunov coefficients recover what was obtained in Ref. 16. Because the results in Ref. 16 were generated via another method (Refs. 12 and 13), this constitutes an excellent validation of our methodology. The effect of the linear control on V_F is depicted in Fig. 2 (as solid lines), whereas the effect on L is shown in Fig. 3. It is noted that the flutter speed monotonically increases with increases of flight Mach numbers M_∞ and/or the control gain Ψ_1. When $L < 0 (>0)$, the corresponding motion is stable (unstable) in the sense of Hopf bifurcation. We can define the value of the Mach number at which $L = 0$ as the critical value M_{TR}, where TR means transitory indicating L is crossing the zero critical value. It can be seen that in general the motions are stable for smaller Mach numbers and unstable for larger Mach numbers. Moreover, it is interesting to observe that the slopes of the curves are slightly decreasing as the Ψ_1 is increasing, suggesting that the M_{TR} is larger for larger values of Ψ_1 and physically giving a measure of the rapidity of transition of the aeroelastic system, from the benign state to the catastrophic one, that is, an idea of the occurrence of a mild or explosive type of flutter.

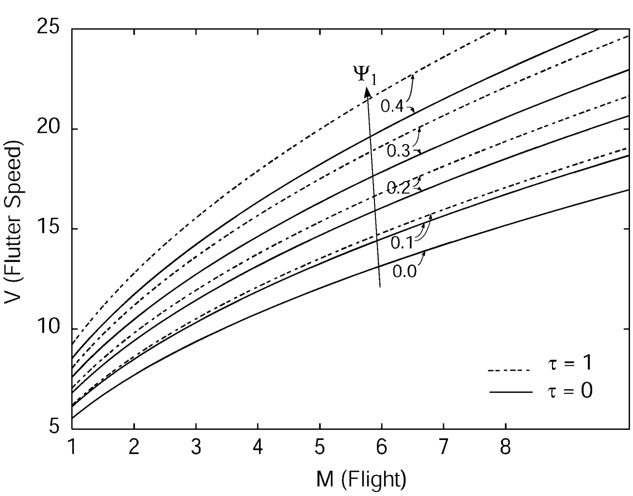

Fig. 2 Effects of the linear control with or without time delay on the flutter boundary.

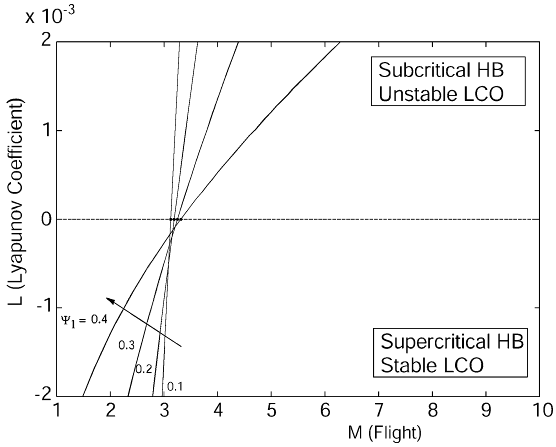

Fig. 3 LFQ corresponding to $\Psi_2 = 0$, $\tau = 0$ for $\Psi_1 = 0.1$, 0.2, 0.3, and 0.4.

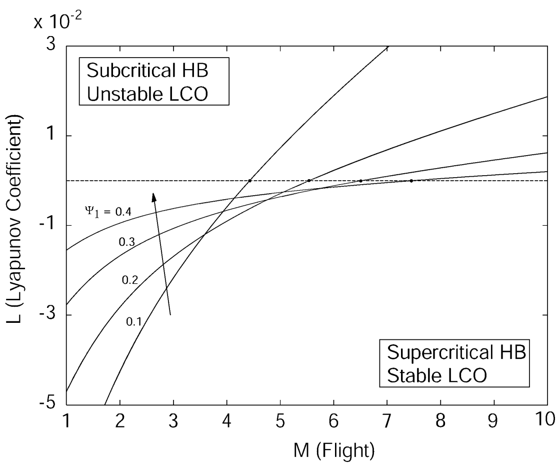

Fig. 4 LFQ corresponding to $\Psi_2 = 10\ \Psi_1$, $\tau = 0$ for $\Psi_1 = 0.1$, 0.2, 0.3, and 0.4.

b) $\Psi_2 = 10\Psi_1$. Here, for convenience in comparison, we take $\Psi_2 = 10\Psi_1$. The presence of Ψ_2 does not change the relation between the flutter velocity and Mach number because the flutter speed is only determined by linear terms. The Lyapunov coefficients for this case are depicted in Fig. 4. This result is also in good agreement with that in Ref. 16. It clearly shows that the nonlinear feedback control is more effective than the linear feedback control in rendering the flutter boundary a benign one.

Case 2: Fixed time delay τ, but Ψ_1 is varied.

First, the time delay τ given in Eqs. (6a–6d) is nondimensionalized. The real time delay is $\hat{\tau} = \tau\omega_\alpha$.

Now we fix the time delay ($\tau = 1$ is selected in this paper) and investigate the effects of the linear and nonlinear control gains on the flutter stability boundary.

a) $\Psi_2 = 0$. The results for considering the linear control only are shown in Figs. 2–5. It is noted from Fig. 2 that the trends are similar to that of the case without time delay. V_F is a monotonically increasing function of the linear control gain Ψ_1 and the flight Mach number M_∞. However, the value of V_F, in the presence of time delay, for any (Ψ_1, M_∞) experiences an increase, as compared to the case of the absence of the time delay. Compared with the case without time delay, it is seen that the effect of τ becomes more prominent for larger values of Ψ_1. This suggests that incorporation of time delay in the feedback control is beneficial to control flutter instability, and a better control can be obtained using a proper combination of time delay with larger linear control gains. Similar trends can also be observed from Fig. 5, where the values of Lyapunov coefficient are shown. Again, comparing this figure with that in Ref. 16 indicates that the time delay helps stabilize vibrating motions.

b) $\Psi_2 = 10\Psi_1$. The results obtained for this case are shown in Fig. 6. The effect of the nonlinear control combined with the linear

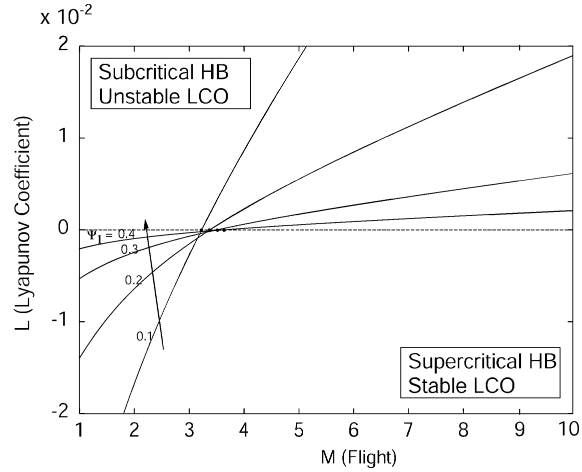

Fig. 5 LFQ corresponding to $\Psi_2 = 0$, $\tau = 1$ for $\Psi_1 = 0.1$, 0.2, 0.3, and 0.4.

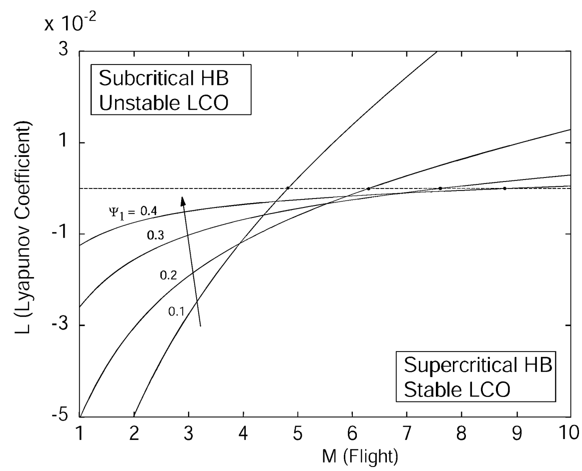

Fig. 6 LFQ corresponding to $\Psi_2 = 10\Psi_1$, $\tau = 1$ for $\Psi_1 = 0.1$, 0.2, 0.3, and 0.4.

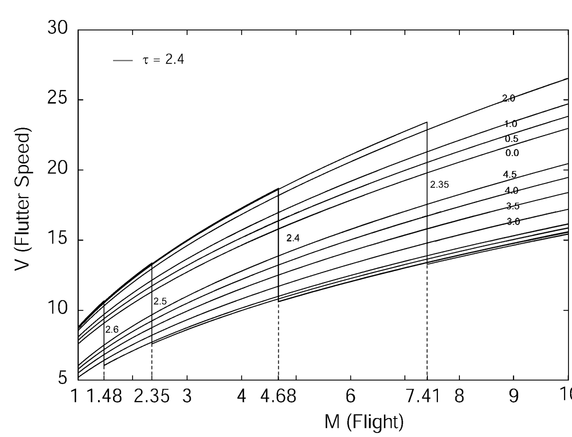

Fig. 7 Effects of the time delay on the flutter boundary for $\Psi_1 = 0.3$ and $\Psi_2 = 0$.

control can be clearly observed from this figure. Further, a comparison among Figs. 4–6 again confirms that time delay and nonlinear control lay much more stress on the stability.

Case 3: Ψ_1 fixed, but $\tau \neq 0$ is varied.

We consider the variation of the time delay τ.

a) $\Psi_2 = 0$. The results are presented in Figs. 7–10, which clearly show that the time delay has significant implications on the character of the flutter boundary and the stability conditions (Lyapunov coefficients).

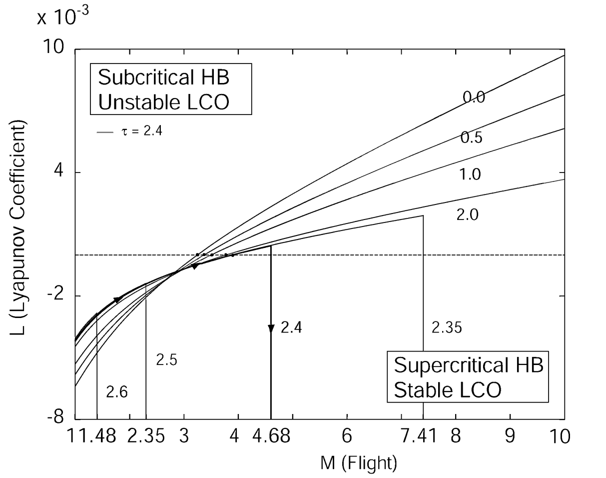

Fig. 8 LFQ corresponding to $\tau = 0.0$, 0.5, 1.0, 2.0, 2.35, 2.4, 2.5, and 2.6 for $\Psi_1 = 0.3$ and $\Psi_2 = 0$.

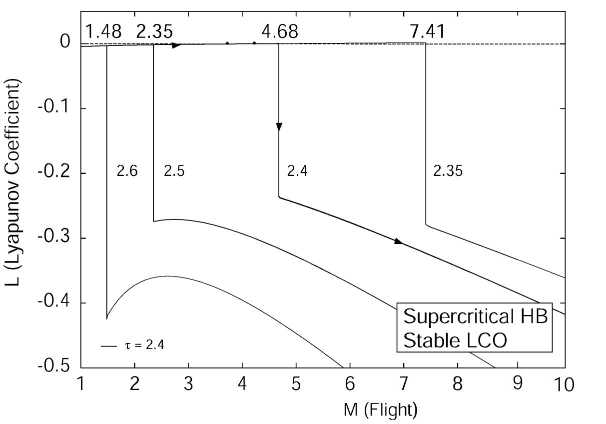

Fig. 9 Jumping part of the LFQ corresponding to $\tau = 2.35$, 2.4, 2.5, and 2.6 for $\Psi_1 = 0.3$ and $\Psi_2 = 0$.

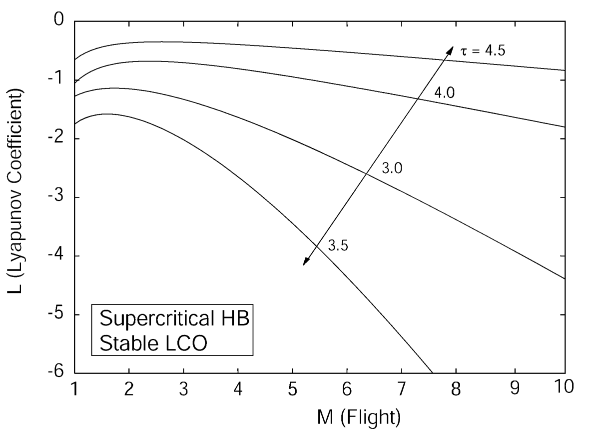

Fig. 10 LFQ corresponding to $\tau = 3.0$, 3.5, 4.0, 4.5 for $\Psi_1 = 0.3$ and $\Psi_2 = 0$.

Figure 7 shows the effect of the time delay on the flutter speed with respect to the variation of the flight Mach number, when Ψ_1 is fixed at $\Psi_1 = 0.3$. The interval of the variation of τ is from 0.0 to 4.5, and the Mach number M_∞ is varied from 1 to 10. The values of the Lyapunov coefficient L, corresponding to the data presented in Fig. 7, are plotted in Figs. 8–10. Note that Fig. 8 shows the results for intermediate values of τ, whereas Figs. 9 and 10 depict the trends of L for large values of τ. The following interesting phenomena have been observed.

i) When $\tau \in [0.0, 2.32]$, the results can be seen from Figs. 7 and 8. In this case, similar trends as those shown in Figs. 2 and 5 are observed: the V_F increases as τ is increasing, thus revealing that the time delay τ ranging in this interval is beneficial in the sense of expanding the flutter envelope. Also, it is seen from Fig. 8 that the motion is more stable for larger values of τ. This suggests that subcase i) is better than in the absence of time delay, case 1a).

ii) When $\tau \geq 2.73$, the trends for the flutter speed are similar to that of subcase i), that is, V_F increases as τ is increasing. However, all values of V_F are less than that of $\tau = 0$, implying that subcase ii) is worse than case 1a), which has no time delay. However, for this case (see Fig. 10) all values of L are less than zero, meaning that all of the corresponding motions are stable. This implies that the application of larger time delay can convert subcritical Hopf bifurcation to supercritical, though it is not good in controlling the initiation of Hopf bifurcation (i.e., the flutter boundary). This apparent conflict suggests that in order for the time delay to be beneficial in controlling the initiation of Hopf bifurcation (delaying the bifurcation) as well as stabilizing the bifurcating limit cycles, one should choose small time delays.

iii) The most interesting effect is observed when $\tau \in (2.33, 2.73)$ on which there exist critical Mach numbers for each value of τ. When the Mach number is less than the critical value, the trends are similar to subcase i); otherwise, they are similar to subcase ii) (see Figs. 8 and 9). For example, when $\tau = 2.35$ the transitory Mach number is $M_{TR} = 7.41$. When $M_\infty < 7.41$, the time delay is beneficial not only in delaying the initiation of Hopf bifurcation (see Fig. 7), but also in stabilizing the bifurcating motions (see Fig. 8). However, when $M_\infty > 7.41$ the values of V_F are less than those corresponding to the case without time delay, as shown in Fig. 7, indicating that the time delay can reduce the flight envelope. However, the Hopf bifurcation is supercritical (see Fig. 9).

From the discussions given in the preceding three subcases, we have found that in general larger values of τ yield more negative values of the Lyapunov coefficients, implying that the time delay is beneficial in stabilizing bifurcating periodic motions. It can be used for control of Hopf bifurcation such that a subcritical Hopf bifurcation is changed to supercritical. More precisely, for small values of τ ($\tau \in [0.0, 2.33]$ in subcase i), see Fig. 8), the bifurcating limit cycles are only stable for small flight Mach numbers because of the detrimental effects of the aerodynamic nonlinearities that build up at increasing Mach flight. For large values of τ ($\tau \geq 2.73$ in subcase iii), see Fig. 10), the periodic motions are stable for any Mach numbers. When $\tau \in (2.33, 2.73)$ (in subcase ii), see Fig. 9), there is a jump of the Lyapunov coefficient at the transitory Mach number M_{TR}, and the Hopf bifurcation solutions become more stable when $M_\infty > M_{TR}$. For different values of time delay τ, the jumps are occurring either from the subcritical to supercritical ranges or completely in the supercritical range. A three-dimensional plotting showing the trend of L with respect to τ and M is given in Fig. 11. It clearly shows the trends observed in Figs. 8–10.

However, it has been observed from Fig. 7 that the effect of the time delay on the initiation of Hopf bifurcation is more complicated

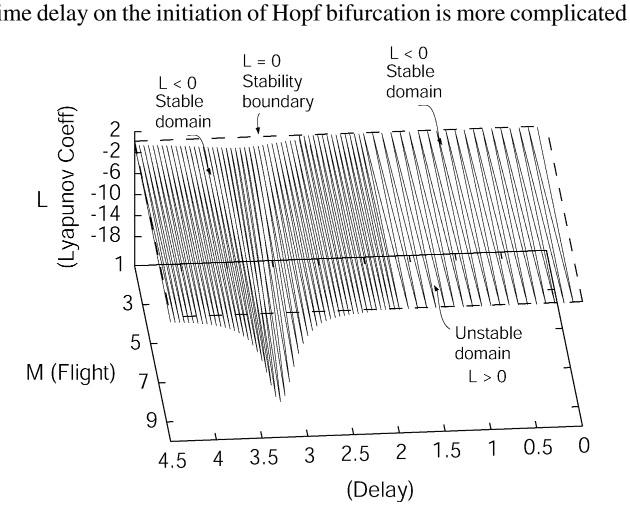

Fig. 11 Three-dimensional plot of L vs τ and M when $\Psi_1 = 0.3$ and $\Psi_2 = 0$.

than the trends of the Lyapunov coefficients. It does not show the trend that larger values of τ are always beneficial in delaying the initiation of Hopf bifurcation. In fact, it has been seen that when the time delay is relatively small ($\tau \in [0.0, 2.33]$) inclusion of the time delay in the feedback control is indeed beneficial to delay Hopf bifurcation. For relatively large time delay ($\tau \geq 2.73$), adding time delay in the control is actually worse than the case without time delay, implying that the time delay helps the initiation of Hopf bifurcation, which should be avoided in design if the object of the control is to delay the occurrence of the flutter instability. For intermediate time delays, [$\tau \in (2.33, 2.73)$], a more complicated phenomenon, namely a snap-through jump from the benign type of flutter ($L < 0$) to the catastrophic one ($L > 0$), is occurring. For each value of τ, there exists a critical value M_{TR} of the Mach number. The time delay is beneficial in controlling the initiation of Hopf bifurcation when $M < M_{\mathrm{TR}}$; otherwise, it is worse than the case without applying time delay.

Therefore, toward controlling both the initiation of Hopf bifurcation and the stability of bifurcating periodic motions, one should apply relatively small values of τ. For the parameter values chosen in this paper, the proper time delay should correspond to $\tau < 2.3$. As the system parameters are changed, this value, certainly will be changed.

b) $\Psi_2 = 10\,\Psi_1$. Now we turn to the case when the nonlinear feedback control is added. The discussions are similar to part a), and we thus omit the details, but present a different trend. Figure 12 shows the values of the Lyapunov coefficients with respect to the variations of τ when $\Psi_1 = 0.3$ and $\Psi_2 = 3$. Comparing Fig. 12 with Fig. 8 clearly shows that the time delay is beneficial in controlling the stability of Hopf bifurcation. For the small values of $\tau = 0.0, 0.5, 1.0$, and 2.0, now the bifurcating motions are stable even for large values of Mach number. For example, consider $\tau = 1.0$. If $\Psi_2 = 0$, the motion for this case is stable when $M < 3.5$, whereas it is stable as long as $M < 7.8$ when $\Psi_2 = 3$. When the time delay takes the intermediate values $\tau = 2.35, 2.4, 2.5$, and 2.6, the trends are different from what was observed in Fig. 8, as discussed in case 3, a) iii) with $\Psi_2 = 0$. Figure 8 shows that all of the motions are stable after the jumping, which occurs at the transitory values of the Mach number. However, now when $\Psi_2 = 3$, as is seen from Fig. 12, because the corresponding values of L jump from negative to positive the motion becomes unstable. This suggests that a combination of the nonlinear control with an intermediate value of τ is not beneficial in controlling the stability of Hopf bifurcation. In fact, it can change a supercritical Hopf bifurcation to subcritical, which is certainly not desirable.

Similarly, we can plot the Lyapunov coefficient in a three-dimensional space as a function of τ and M. The results corresponding to those presented in Fig. 12 are shown in Fig. 13. It clearly appears that for small values of the time delay ($\tau < 2$), $L < 0$, and thus the limit cycle is stable. However, for relatively large values of the time delay ($\tau > 2$), $L > 0$, and thus the motions are unstable, which contradicts the trends observed from Fig. 11 where nonlinear control is not applied.

From the results obtained in parts a) and b) of case 3, we can conclude that in order to best use the nonlinear feedback control, combined with the time delay, relatively small values of the time delay should be used.

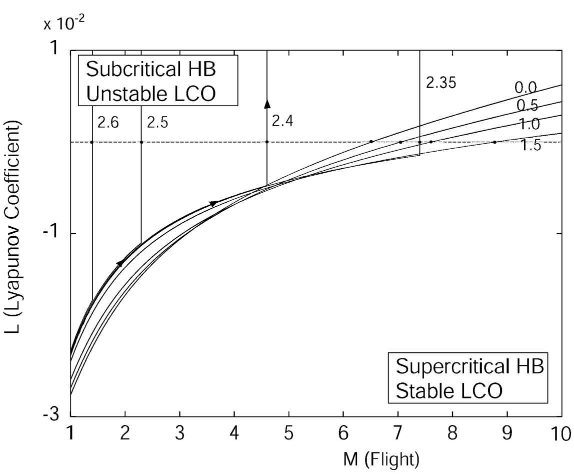

Fig. 12 LFQ corresponding to $\Psi_2 = 10\Psi_1$ and $\Psi_1 = 0.3$, for $\tau = 0.0$, 0.5, 1.0, 2.0, 2.35, 2.4, 2.5, and 2.6.

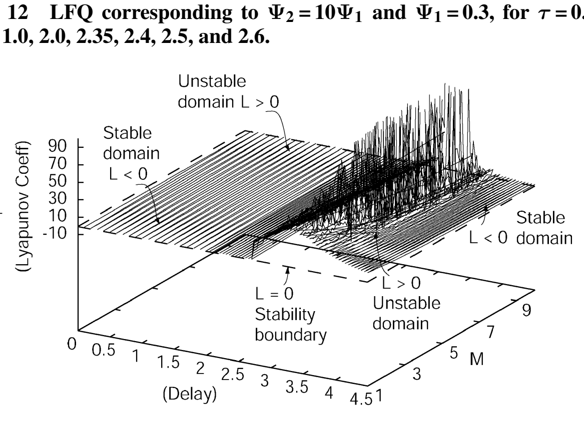

Fig. 13 Three-dimensional plot of L vs τ and M when $\Psi_1 = 0.3$ and $\Psi_2 = 3$.

Conclusions

The aeroelastic instability in the vicinity of the flutter boundary for a two-dimensional supersonic lifting surface is addressed. Particular attention is focused on the effect of the time-delayed feedback control on flutter instability boundary and its character (benign/catastrophic). Bifurcations into limit cycles (Hopf bifurcation) are investigated with respect to system parameters as well as the time delay. Center manifold reduction and normal form theory are applied to simplify the analysis and reduce the original system to a two-dimensional center manifold. Then, the predictions of the stability conditions for bifurcation solutions are obtained. Numerical results are also presented to show the effects of the time delay and the linear/nonlinear feedback control gains. In particular, the initiation of Hopf bifurcation and the stability of bifurcating periodic motions are studied in detail. It has been shown that inclusion of a linear feedback control is always beneficial in controlling both the initiation of Hopf bifurcation and the stability of motions, regardless of the inclusion or noninclusion of the time delay. The presence of a time delay into the nonlinear feedback control can have a profound effect on the stability of the bifurcating motions. It can transfer subcritical Hopf bifurcations (occurring in the presence of aerodynamic nonlinearities) to supercritical. It has been shown that the effect of the time delay becomes more prominent for large linear control gains. However, it has been found that larger time delays are not beneficial in delaying Hopf bifurcation. When nonlinear feedback control is applied, the situation becomes even more complicated. It can destabilize the bifurcating motions (i.e., changing supercritical Hopf bifurcation to subcritical) if the nonlinear control is combined with larger time delay. Therefore, based on the results obtained in this paper, to obtain the best controller in controlling both the initiation of Hopf bifurcation and the stability of bifurcating motions one should apply both linear and nonlinear controls with small time delay. Further studies, based on the center manifold reduction and numerical simulations, will be given to consider the system with damping, as well as higher codimensional singularities such as double Hopf bifurcation and combination of Hopf bifurcation and zero singularity.

Appendix A: Expressions of the Coefficients Appearing in Eqs. (6)

$$a_1 = -\frac{\bar{\omega}^2 r_\alpha^2}{V^2\left(r_\alpha^2 - \chi_\alpha^2\right)} \tag{A1}$$

$$a_2 = \frac{1}{r_\alpha^2 - \chi_\alpha^2}\left(\frac{\chi_\alpha r_\alpha^2}{V^2} - \frac{\gamma x_{\mathrm{ea}}\chi_\alpha}{b\mu M_\infty} + \frac{\gamma\chi_\alpha}{\mu M_\infty} - \frac{\gamma r_\alpha^2}{\mu M_\infty}\right) \tag{A2}$$

$$a_3 = \frac{1}{r_\alpha^2 - \chi_\alpha^2}\left(\frac{\chi_\alpha\gamma x_{\mathrm{ea}}}{b\mu M_\infty} - \frac{\gamma\chi_\alpha}{\mu M_\infty} - \frac{\gamma r_\alpha^2}{\mu M_\infty} - \frac{2\xi_h\bar{\omega} r_\alpha^2}{V}\right) \tag{A3}$$

$$a_4 = \frac{1}{r_\alpha^2 - \chi_\alpha^2}\left(\frac{2\chi_\alpha \gamma x_{\mathrm{ea}}}{b\mu M_\infty} + \frac{2\chi_\alpha \xi_\alpha r_\alpha^2}{V} + \frac{\gamma x_{\mathrm{ea}} r_\alpha^2}{b\mu M_\infty} - \frac{4\gamma\chi_\alpha}{3\mu M_\infty} - \frac{\gamma r_\alpha^2}{\mu M_\infty} - \frac{\chi_\alpha \gamma x_{\mathrm{ea}}^2}{b^2\mu M_\infty}\right) \tag{A4}$$

$$a_5 = \frac{1}{r_\alpha^2 - \chi_\alpha^2}\left[\frac{\chi_\alpha B r_\alpha^2}{V^2} + \frac{\chi_\alpha M_\infty \gamma^3 \delta_A x_{\mathrm{ea}}(1+\kappa)}{12b\mu} - \frac{\gamma^3\delta_A M_\infty\left(\chi_\alpha + r_\alpha^2\right)(1+\kappa)}{12\mu}\right] \tag{A5}$$

$$e_1 = \frac{\Psi_1 \chi_\alpha r_\alpha^2}{V^2\left(r_\alpha^2 - \chi_\alpha^2\right)} \tag{A6}$$

$$e_2 = \frac{\Psi_2 \chi_\alpha r_\alpha^2}{V^2\left(r_\alpha^2 - \chi_\alpha^2\right)} \tag{A7}$$

$$b_1 = \frac{\bar{\omega}^2 \chi_\alpha}{V^2\left(r_\alpha^2 - \chi_\alpha^2\right)} \tag{A8}$$

$$b_2 = \frac{1}{r_\alpha^2 - \chi_\alpha^2}\left(\frac{\chi_\alpha\gamma}{\mu M_\infty} - \frac{\gamma}{\mu M_\infty} + \frac{\gamma x_{\mathrm{ea}}}{\mu M_\infty b} - \frac{r_\alpha^2}{V^2}\right) \tag{A9}$$

$$b_3 = \frac{1}{r_\alpha^2 - \chi_\alpha^2}\left(\frac{\chi_\alpha\gamma}{\mu M_\infty} + \frac{\gamma}{\mu M_\infty} + \frac{2\chi_\alpha \xi_h \bar{\omega}}{V} - \frac{\gamma x_{\mathrm{ea}}}{b\mu M_\infty}\right) \tag{A10}$$

$$b_4 = \frac{1}{r_\alpha^2 - \chi_\alpha^2}\left(\frac{4\gamma}{3\mu M_\infty} + \frac{\gamma\chi_\alpha}{\mu M_\infty} + \frac{\gamma x_{\mathrm{ea}}^2}{b^2\mu M_\infty} - \frac{2\gamma x_{\mathrm{ea}}}{b\mu M_\infty} - \frac{2\xi_\alpha r_\alpha^2}{V} - \frac{\gamma x_{\mathrm{ea}}\chi_\alpha}{b\mu M_\infty}\right) \tag{A11}$$

$$b_5 = \frac{1}{r_\alpha^2 - \chi_\alpha^2}\left[\frac{\gamma^3\delta_A M_\infty(\chi_\alpha + 1)(1+\kappa)}{12\mu} - \frac{B r_\alpha^2}{V^2} - \frac{M_\infty\gamma^3\delta_A x_{\mathrm{ea}}(1+\kappa)}{12b\mu}\right] \tag{A12}$$

$$f_1 = -\frac{\Psi_1 r_\alpha^2}{V^2\left(r_\alpha^2 - \chi_\alpha^2\right)} \tag{A13}$$

$$f_2 = -\frac{\Psi_2 r_\alpha^2}{V^2\left(r_\alpha^2 - \chi_\alpha^2\right)} \tag{A14}$$

Appendix B: Expressions of the Coefficients Appearing in Eqs. (24) and (26)

$$L_1 = e_1 f_1 \omega^4 + [f_1 a_4(e_1 b_3 - a_3 f_1) + e_1 b_4(a_3 b_1 - b_3 e_1) + e_1(f_1 b_2 - b_1 e_1 + f_1(a_1 e_1 - a_2 f_1)]\omega^2 + (b_2 e_1 - a_2 f_1)(a_1 f_1 - b_1 e_1) \tag{B1}$$

$$L_2 = [e_1(b_3 e_1 - a_3 f_1) + f_1(e_1 b_4 - a_4 f_1)]\omega^2 + (a_3 f_1 - b_3 e_1)(f_1 a_2 - e_1 b_2) + (a_4 f_1 - b_4 e_1)(e_1 b_1 - f_1 a_1) \tag{B2}$$

$$L_0 = e_1^2\omega^4 + \left[(f_1 a_4 - e_1 b_4)^2 + 2e_1(e_1 b_2 - f_1 a_2)\right]\omega^2 + (f_1 a_2 - e_1 b_2)^2 \tag{B3}$$

$$L_3 = -(a_1 M_2 N_1 + \omega M_3 N_2) \tag{B4}$$

$$L_4 = a_1 M_2 N_2 - \omega M_3 N_1 \tag{B5}$$

$$L_5 = \omega(M + a_4 M_2)N_2 + (a_4 M_1 - b_4 M)N_1 \tag{B6}$$

$$L_6 = \omega(M + a_4 M_2)N_1 - (a_4 M_1 - b_4 M)N_2 \tag{B7}$$

$$L_7 = -(M_1 N_1 + \omega M_2 N_2) \tag{B8}$$

$$L_8 = -\omega M_2 N_1 + M_1 N_2 \tag{B9}$$

$$M = \left(\omega^2 + a_1^2\right)^2 + \omega^2 a_3^2 \tag{B10}$$

$$M_1 = (b_1 + a_3 b_3)\omega^2 + a_1 b_1 \tag{B11}$$

$$M_2 = b_3\omega^2 + a_1 b_3 - a_3 b_1 \tag{B12}$$

$$M_3 = b_1\omega^2 + a_3(b_1 a_3 - b_3 a_1) + a_1 b_1 \tag{B13}$$

Acknowledgments

Y. Yuan and P. Yu thank the support received from the Natural Sciences and Engineering Research Council of Canada (Grant No. G26135703, R2686A02). L. Librescu and P. Marzocca gratefully acknowledge the partial support of this research by the NASA Langley Research Center through Grant NAG-1-02-011.

References

[1]Mukhopadhyay, V. (ed.), "Benchmark Active Control Technology," *Journal of Guidance, Control, and Dynamics*, Pt. I, Vol. 23, No. 5, 2000, pp. 913–960; Pt. II, Vol. 23, No. 6, 2000, pp. 1093–1139; Pt. III, Vol. 24, No. 1, 2001, pp. 146–192.

[2]Mukhopadhyay, V., "Flutter Suppression Control Law Design and Testing for the Active Flexible Wing," *Journal of Aircraft*, Vol. 32, No. 1, 1995, pp. 45–51.

[3]Yuan, Y., Yu, P., Librescu, L., and Marzocca, P., "Analysis of a 2-D Supersonic Lifting Surface with Time Delayed Feedback Control," *2003 AIAA Dynamics Specialists Conference Proceedings* [CD-ROM], AIAA, Reston, VA, 2003.

[4]Guckenheimer, J., and Holmes, P., *Nonlinear Oscillations, Dynamical Systems, and Bifurcations of Vector Fields*, 4th ed., Springer-Verlag, New York, 1993, Chap. 3.

[5]Marsden, J. E., and McCracken, M., *The Hopf Bifurcation and Its Applications*, Springer-Verlag, New York, 1976.

[6]Yu, P., "Computation of Normal Forms via a Perturbation Technique," *Journal of Sound and Vibration*, Vol. 211, 1998, pp. 19–38.

[7]Chen, G., Moiola, J. L., and Wang, H. O., "Bifurcation Control: Theories, Methods, and Applications," *International Journal of Bifurcation and Chaos*, Vol. 10, 2000, pp. 511–548.

[8]Calandrini, G., Paolini, E., Moiola, J. L., and Chen, G., "Controlling Limit Cycles and Bifurcations," *Controlling Chaos and Bifurcations in Engineering Systems*, edited by G. Chen, CRC Press, Boca Raton, FL, 1999, pp. 200–227.

[9]Yu, P., and Chen, G., "Hopf Bifurcation Control Using Nonlinear Feedback with Polynomial Function," *International Journal of Bifurcation and Chaos*, Vol. 14, No. 5, Jan. 2004.

[10]Librescu, L., Chiocchia, G., and Marzocca, P., "Implications of Cubic Physical/Aerodynamic Nonlinearities on the Character of the Flutter Instability Boundary," *International Journal of Non-Linear Mechanics*, Vol. 38, No. 3, 2003, pp. 173–199.

[11]Marzocca, P., Librescu, L., and Silva, W. A., "Flutter, Post-Flutter and Control of a Supersonic 2-D Lifting Surface," *Journal of Guidance, Control, and Dynamics*, Vol. 25, No. 5, 2002, pp. 962–970.

[12]Librescu, L., "Aeroelastic Stability of Orthotropic Heterogeneous Thin Panels in the Vicinity of the Flutter Critical Boundary–Part I and Part II," *Journal de Mécanique*, Vol. 4, No. 1, 1965, pp. 51–76; Vol. 6, No. 1, 1966, pp. 133–152.

[13]Librescu, L., *Elastostatics and Kinetics of Anisotropic and Heterogeneous Shell-Type Structures*, Noordhoff, Leyden, The Netherlands, 1975, Chap. 1 and Appendix A.

[14]Liu, D. D., Yao, Z. X., Sarhaddi, D., and Chavez, F. R., "From Piston Theory to a Unified Hypersonic-Supersonic Lifting Surface Method," *Journal of Aircraft*, Vol. 34, No. 3, 1997, pp. 304–312.

[15]Thuruthimattam, B. J., Friedmann, P. P., McNamara, J. J., and Powell, K. G., "Aeroelasticity of a Generic Hypersonic Vehicle," AIAA Paper 2002-1209, April 2002.

[16]Marzocca, P., Librescu, L., and Silva, W. A., "Supersonic Flutter and Post-Flutter Active Control of Cross-Sectional Aircraft Wings," International Council of the Aeronautical Sciences, Sept. 2002.

[17]Ramesh, M., and Narayanan, S., "Controlling Chaotic Motion in a Two-Dimensional Airfoil Using Time-Delayed Feedback," *Journal of Sound and Vibration*, Vol. 239, No. 5, 2001, pp. 1037–1049.

[18]Yu, P., Yuan, Y., and Xu, J., "Study of Double Hopf Bifurcation and Chaos for an Oscillator with Time Delayed Feedback," *International Journal of Communications in Nonlinear Science and Numerical Simulation*, Vol. 7, No. 1–2, 2002, pp. 69–91.